SAXS STUDY ON THE STRUCTURE AND CRYSTALLIZATION OF AMORPHOUS METALLIC ALLOYS

Supplement to Sci. Rep. RITU, A, March, 1980

SAXS STUDY ON THE STRUCTURE AND CRYSTALLIZATION OF AMORPHOUS METALLIC ALLOYS

K. Osamura, K. Shibue, R. Suzuki and Y. Murakami

Department of Metallurgy, Kyoto University,

606 Kyoto, Japan

INTRODUCTION

The question of atomic configurations in amorphous alloys has received much attention in recent years, with particular interest being directed towards the local order in the materials. Up to now, much informations mainly on nearest neighbours are accumlated by several experimental techniques as wide angle diffraction study and Mössbauer spectroscopy and so on. On the other hand, transmission electron microscopy has been performed in order to clarify the structure of as-splatted amorphous alloy as well as that of subsequently aged specimens. It is, however, difficult to determine quantitatively the nature of the inhomogeneity in materials on a fine scale in the order of several nm or less. The small angle scattering (SAS) measurements [1,2,3] are very effective on such a fine scale to gain quantitative information concerning the size, distribution and character of the scattering regions.

In the present work, we carried out SAXS intensity measurements as well as the transmission electron microscope (TEM) observation for several amorphous alloys as Fe-P-C, Fe-B, Pd-Si and Pd-Au-Si alloys and analyzed the results in order to obtain structural information in the amorphous state and during the crystallization process.

EXPERIMENTAL METHODS

The amorphous alloys investigated here were made by the ordinary single drum technique. The chemical composition of the prepared ribbons were Fe-10.4at%P-6.3at%C, Fe-17at%B, Pd-18at%Si and Pd-6at%Au-18at%Si. The SAXS intensity for the amorphous alloys was measured in transmission geometry with a Kratky camera as mentioned in detail in our previous report [1]. Mo radiation was generated by a Rigaku power supply RU200PL operated at 50 kV and 160 mA. The measured intensity $\tilde{J}(s)$ was desmeared using a computer program. The desmeared intensity, I(s) was then placed on an absolute basis by comparison with the scattering intensity measured for a known standard material under the same conditions. The standard material used for this purpose was a polyethylene. Also in order to check the structural change during isother-

mal ageing, the diffraction intensity was measured over a wide rage of scattering angles in the transmission geometry and the TEM observation was performed.

EXPERIMENTAL RESULTS AND DISCUSSION

a. Structure of amorphous phase

Some typical examples of SAXS intensity from the amorphous alloys are presented as follows. For those alloys, no crystalline phase was observed and only hallo patterns existed on the TEM photographs. Fig. 1 shows the angular dependence of SAXS intensity increased gradually during ageing suggesting the occurrence of a change of atomic configuration within the amorphous state. For X-ray diffraction in materials, the electron density-density correlation is given by the equation,

$$\gamma(\vec{r}) = \int_V \Delta\rho(\vec{r}_1)\,\Delta\rho(\vec{r}_1 + \vec{r})\,d\vec{r}_1 \qquad (1)$$

where $\Delta\rho(r)$ is the fluctuation of electron density at position $\vec{r}$. The above function will simply be called the " correlation function" hereafter. When a centre of symmetry exists, the correlation function can be directly obtained from the observed intensity, I(s) without any structural assumption as follows;

$$\gamma(r) = (2\pi^2 r)^{-1}\int_0^\infty s\, I(s)\, \sin(sr)\, ds \qquad (2)$$

At r = 0, the function has a special meaning and is usually called the " integrated intensity",

$$\gamma(0) = (8\pi^3)^{-1}\int_0^\infty 4\pi s^2 I(s)\, ds = \langle\Delta\rho^2\rangle V_f\,(1 - V_f) \qquad (3)$$

where $\langle\Delta\rho^2\rangle$ is the square mean fluctuation of electrondensity over the whole system and V_f is the volume fraction. Fig. 2 shows the experimental results calculated by Eq.(2). The correlation seemed to be divided into two parts. A first part is the strong and rapidly decreasing correlation from the origin. The radial distance corresponding to zero correlation was determined by extrapolating the slope around the origin, to yield an average dimension of the scattering region. Its value was 1.8 nm for the as-splatted specimen, and remained nearly constant at 2.0 to 2.4 nm for the aged specimens. Second characteristic feature is the rather week long-distance correlation was established and increased during ageing.

Whithin the amorphous state of Fe-B alloy, the discernible change in SAXS intensity was also observed during isothermal ageing at 546 K as shown in Fig. 3. The intensity increased after ageing for short period and the angular dependence of intensities for aged specimens up to 300 Ks is similar each other. The large scattering intensity of the 1.92 Ms aged specimen is caused by the precipitation of crystalline particles. The corresponding correlation is shown in Fig. 4. In general, its radial distance dependence is quite similar to that for the Fe-P-C alloys, where the small region of electron density fluctuation was suggested to present in the amorphous state.

As defined in Eq.(2), the correlation function provides only the information in the vector space of $\Delta\rho(\vec{r})$. So we must deduce a reasonable structure of amorphous state from the observed density-density correlation. Here the above mentioned scattering regions are assumed as particles. There are N particles in the unit volume and each particle possesses a center of symmerty. The correlation function might be epressed explicitly by the equation instead of Eq. (2),

$$\gamma(\vec{r}) = N\int_V \Delta\rho(\vec{r}_1)\ \Delta\rho(\vec{r}_1 + \vec{r})\ d\vec{r}_1 + \sum_k \sum_{j\neq k} \int_V \Delta\rho(\vec{r}_{k1})\ \Delta\rho(\vec{r}_{k1} + \vec{r} + \vec{R}_k - \vec{R}_j)\ d\vec{r}_{k1} \qquad (4)$$

where $\vec{R}_k$ is the vector showing the center of the k-th particle, $\vec{r}_{k1}$ is the vector to a position 1 from the center of the particle and $\vec{r}$ is given as $(\vec{R}_k + \vec{r}_{k1}) - (\vec{R}_j + \vec{r}_{jm})$. The first term means the intra-particle correlation for each particle and the second term shows the inter-particle correlation among different particles. It is difficult to solve analytically the above expression without a structural model. Especially the relative position among particles, $\vec{R}_j - \vec{R}_k$, is usually an unknown function. Here a simple one dimensional model is proposed in order to understand the observed correlation as shown in Figs. 2 and 4.

One dimensional model on the structure of amorphous phase is shown in Fig. 5(a). The small region of diameter D das an electron density fluctuation of $\Delta\rho$. Same regions are distributed randomly in the system, but the nearest neighbours do not come inside beyond a distence R. Owing to the randomness and the averaging towards the long distance, the electron density fluctuation decreases exponetially as a function of radial distance. The above argument is expressed as follows,

$$\Delta\rho(r) = \begin{cases} \Delta\rho & \text{for} \quad -D/2 \leq r_1 \leq D/2 \\ 0 & \text{for} \quad |r_1| > D/2 \end{cases} \qquad (5)$$

$$\sum_k \sum_{j\neq k} \Delta\rho(r_{k1} + r + R_k - R_j) = \begin{cases} N\Delta\rho A \exp -K_1(r_1 + r) & \text{for} \quad |r_1 + r| > R \\ 0 & \text{for} \quad -R < r_1 + r < R \end{cases} \qquad (6)$$

Substituting Eqs. (5) and (6) into Eq. (4), from the first term,

$$\gamma_1(r) = N\,(\Delta\rho)^2\,(D - r)/D \qquad (7)$$

from the second term,

$$\gamma_2(r) = \begin{cases} 0 & \text{for} \quad r \leq R - D/2 \\ N(\Delta\rho)^2 K_1^{-1} A \left\{\exp(-K_1 R) - \exp\left[-K_1(r + D/2)\right]\right\} & \text{for} \quad R - D/2 \leq r \leq R + D/2 \end{cases} \qquad (8)$$

$$\left\{ N(\Delta\rho)^2 A K_1^{-1} \left\{ \exp(K_1 D/2) - \exp(-K_1 D/2) \right\} \exp(-K_1 r) \right.$$

$$\text{for} \quad R + D/2 \leq r$$

A schematic representation of Eqs. (7) and (8) is drawn in Fig. 5(b). This behavior can explain well the characteristic feature of the observed correlation shown in Figs. 2 and 4. Therefore the experimental data were analyzed by using the expressions of Eqs.(7) and (8) to obtain some structural parameters. The result is listed in Table 1, where R + D/2 means the nearest neighbour distance from the model. For the as-splatted specimen, for example, the diameter of fluctuated region is 1.2 nm and the nearest neighbour distance is 1.6 nm. This means that the electron density fluctuation occurs very closely in real space. When the alloy was aged, its diameter decreased and the nearest neighbour distance increased for short aging period, but hereafter remain nearly constant. The exponetial term in Eq.(6) indicates the randomness of the arrangement of those regions. The larger value of K_1 means the increasing randomness. During isothermal ageing, it was found out that K_1 increased gradually. But the integrated intensity did not change so much through the isothermal ageing comparing with that of the as-splatted state. A simple and consistent explanation of the above features on structure is that at the as-splatted state, $\Delta\rho$ is small, but V_f is large, and during ageing for short period, $\Delta\rho$ increases, but V_f decreases and their structural change tends to go into a metastable state.

The electron density fluctuation in the amorphous state might originate from two alternative structural inhomogeneities. One is the compositional fluctuation. The rearrangement of metalloid atoms is essentially important. Another inhomogeneity comes from the fluctuation of number density. When small closed packed or local order regions are mixed in less closed or less order ones, an electron density fluctuation can be also expected. Here the packing manner of matallic atoms plays an important role. A possible structure is proposed as follows on the Fe-B alloys [4]. When the molecular unit with composition of Fe_3B is formed and their units pack together to form the glass and the Fe atoms fill the space between units, the expected integrated intensity for $Fe_{83}B_{17}$ alloy is given by

$$\gamma(0) = 0.0067 \times 10^{48} \text{ eu/cm}^6 \qquad (9)$$

For the as-splatted specimen, the experimental value is 0.0066×10^{48} eu/cm^6 and fairly in agreements with the above estimated value. However, the effects contributed to SAXS intensity as the change of number density and the Laue monotonic scattering should be taken into further discussion.

The SAXS intensity was also observed in the $Pd_{76}Au_6Si_{18}$ amorphous alloy as shown in Fig. 6. The angular dependence of the intensity little a bit different from two former cases for Fe-P-C and Fe-B alloys. At the low scattering angle, the intensity rather small. The broad and week maximum appeared around 0.3 nm^{-1}. The ageing time dependence of the intensity was not remarkable. So we might recognize the essential difference on the structure from the above mentioned structure model.

b. Crystallization

Fig.7 shows the angular dependence of SAXS intensity for the aged Fe-10.4at%P-6.3at%C alloy at 663 K, which is lower by about 20 K than its crystallization temperature. The scattering intensity seemed to be divided into two parts. A first part appears in the lower scattering angle region with a characteristic of monotonically decreasing intensity as presented typically in the cases of as-splatted and 50 min aging specimens. The second part corresponds to the shoulder which appears at higher scattering angle region. Its shoulder is related to the micro crystalline phase. The TEM observation was performed on the same specimens used for the SAXS measurement. Fig.8 shows the typical structure which appeared during ageing for 200 min at 663 K. Each crystalline particle exhibited a lamellar structure and very similar to an " axialite" grown from polymer fluid. These alternate phases were confirmed to be Fe_3P and α Fe by the analysis of diffraction patterns. The three dimensional structure of these crystalline particles deducible from the observed two dimensional pictures was the cylindric accumlation of fine lamellae. The regular packing existed only locally and did not occur over the entire particle. A sketch of such regularly piled lamellae is shown in Fig.9. When it was assumed that the closest packing of lamellae occurs in the x-direction and the dimensions of the other (y and z) directions are fairly large, the two different types of analysis of SAXS intensity as given below, give us the size parameters, D and L.

According to Porod[5], the scattering intensity from the one dimensional lamellar packing, where the central separation of neighbouring lamellae with an equal thickneaa, D, has a Gaussian fluctuation, is given by

$$I(s) = \frac{2K\,(1 - D)}{Ds^2} \cdot \frac{1 - \cos(sD)}{[1 - \cos(sD)]^2 + [s(1 - D) + \sin(sD)]^2} \tag{10}$$

where K is a constant. Fig.10 shows the calculated relative change of $s^2I(s)$ based on the structural model shown in Fig.9 as a function of $sD/2\pi$ for some cases with different L/D ratios. In the same figure, the observed result was plotted. The experimental data corresponds well with the calculated curve for L/D = 17.0/5.0. The other analytical results are listed in Table 2.

The observed correlation function for these specimens is shown in Fig.11. Their radial dependence of correlation decreased rapidly at first near the origin and had a weak broadened maximum in the region of 10 to 20 nm. For a lamellar with thickness D, the correlation function is represented as

$$\gamma(r) = \langle \Delta\rho^2 \rangle D\,[1 - (r/D)] \tag{11}$$

From the slope near the origin, the average thickness of lamellae was obtained. The distance to the maximum gave an average nearest neighbour distance L among lamellae. As seen from Table 2, the present results matched fairly well the calculations obtained from Porod's theory. From TEM observation, the smallest D and the closest L were determined to be about 4 and 13 nm, respectively.

The angular dependence of SAXS intensity for the aged Fe-17at%B alloy at 595 K is shown in Fig. 12. The large SAXS intensities for the alloys aged beyond 30 ks are corresponding to small α iron particles [6]. The Guinier radius was obtained to be 6.6 and 10.7 nm for 30 ks and 6 Ms ageing , respectively.

Fig.13 shows the change of SAXS intensity during isothermal ageing at 653 K for the $Pd_{76}Au_6Si_{18}$ alloys. The increasing intensity with ageing time is related to the crystallization of α phase. As shown in Fig. 14, α phase formed during ageing at 653 K is very fine and homogeneously distributed. From the pattern analysis, the matrix remains in the amorphous state. The size of those fine crystals were obtained from both the SAXS intensity and TEM observation as listed in Table 3. The number of particles per unit volume was estimated constantly about 2 to 4 $\times 10^{16}$ cm^{-1} for 653 K ageing.

SUMMARY

The change in structure of several amorphous alloys as Fe-P-C, Fe-B, Pd-Si and Pd-Au-Si alloys during isothermal ageing was examined using small angle X-ray scattering measurement and transmission electron microscopy. The SAXS intensity was related to two different types of scattering sources depending on ageing time and temperature. For the as-splatted amorphous alloys and the specimens aged for short period at the temperature below their crystallization temperatures, the week and spreaded SAXS intensity was observed.This indicates the existence of electron density fluctuation in the amorphous state. The average size of their scattering regions was 1.8 to 2.4 nm for Fe-P-C alloys and 1.2 to 0.8 nm for Fe-B alloys. The origin of its fluctuation has been discussed based on one dimensional model. When the amorphous alloys was aged for longer period, the fine crystalline particles precipitate ; those are the two phase lamellar structure of Fe_3P and α Fe for Fe-P-C alloys, the α iron phase for Fe-B alloys and the α phase for Pd-Au-Si alloys, respectively. Their size and structure were determined from the analysis of SAXS intensity and TEM observation.

References

[1] K.Osamura, K.Shibue, P.H.Shingu and Y. Murakami: J. Mat. Sci., 14(1979)945.
[2] C.P.P.Chou and D. Turnbull: J. Non-Crystalline Solids, 17(1975)169.
[3] J.L.Walter, D.G.Legrand and F.E.Luborsky: Mat. Sci. Eng., 2(1977)161.
[4] D.S.Boudreaux: Phys. Rev. B, 18(1978)4039.
[5] G. Porod: Kolloid Z., 124(1951)83.
[6] J.L.Walter, S.F.Bartram and I.Mella: Tech. Inform. Series, General Elec. Co., 78CRD105, (1978)1.

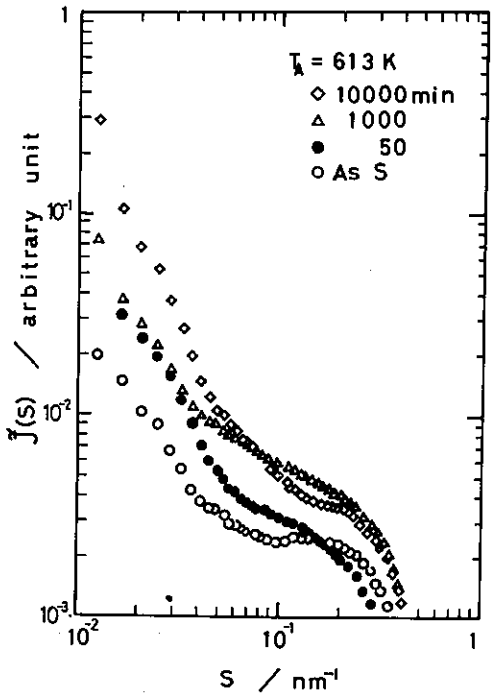

Fig.1 Change of SAXS intensity during ageing at 613 K in Fe-P-C alloys.

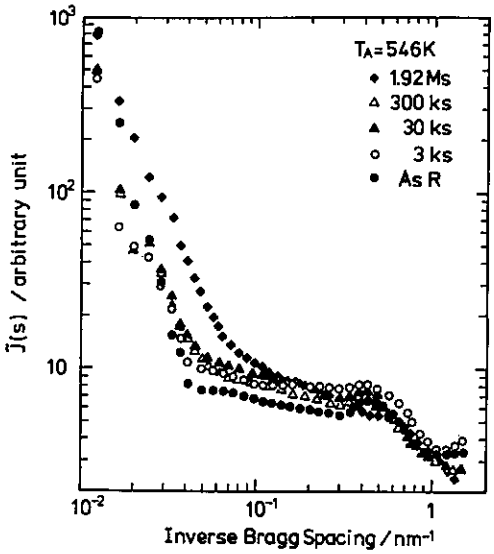

Fig.3 Change of SAXS intensity during ageing at 546 K in Fe-B alloys.

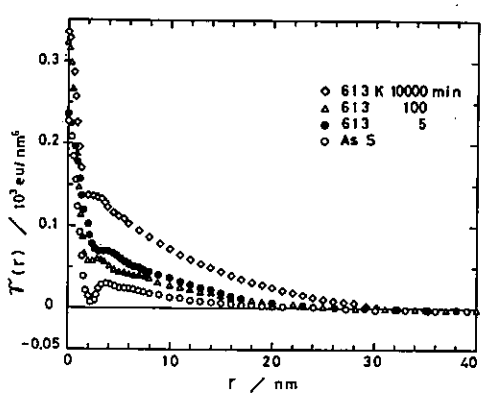

Fig.2 Correlation function in Fe-P-C alloys aged at 613 K.

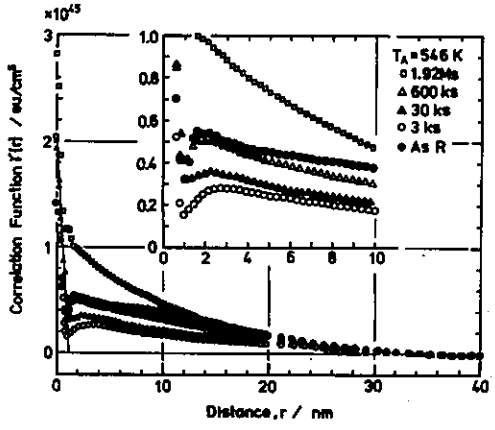

Fig.4 Correlation function in Fe-B alloys aged at 546 K.

Table 1 Summary on the structure analysis of an Fe-B amorphous alloy, where specimens were aged at 546 K.

Ageing Time	D /nm	R /nm	K_1	A
as-splatted	1.2	1.0	3.8×10^{-3}	4.09×10^{-2}
600 s	0.8	1.8	4.9	2.38
3 ks	0.8	1.8	6.1	2.97
30 ks	0.9	1.8	6.7	3.10
300 ks	1.0	2.0	6.7	3.29
1.92 Ms	-	-	6.8	-

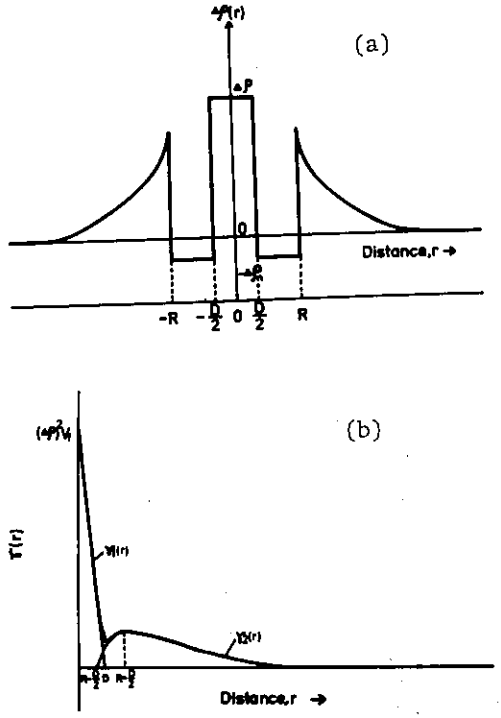

Fig.5 (a) A proposed reduced structure of amorphous phase.
(b) The corresponding correlation function.

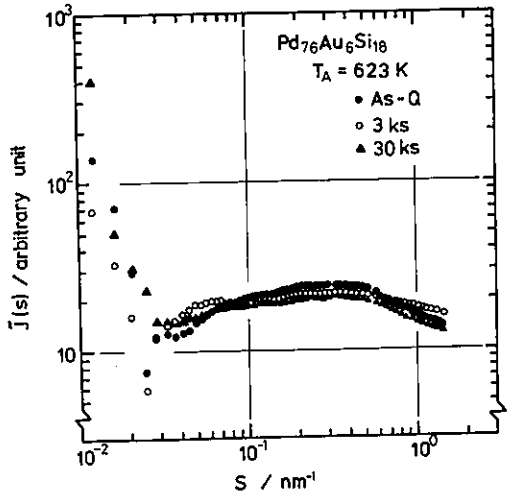

Fig.6 Change of SAXS intensity during ageing at 623 K in Pd-Au-Si alloys.

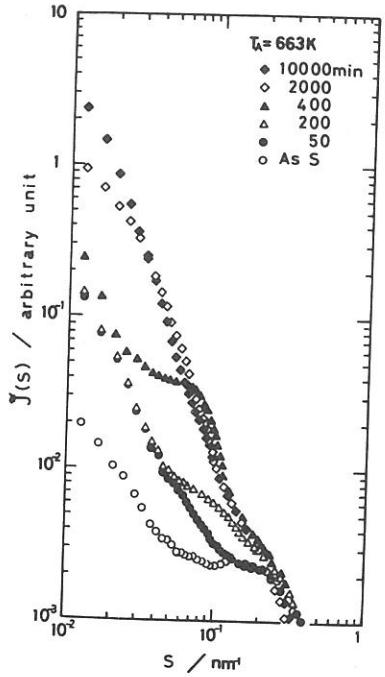

Fig.7 Change of SAXS intensity during ageing at 663 K in Fe-P-C alloys.

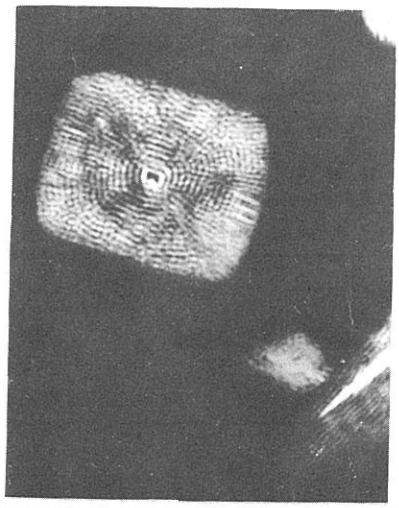

Fig.8 TEM photograph for the aged Fe-P-C alloy at 663 K for 200 min. (x60,000)

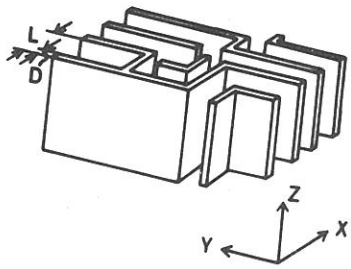

Fig.9 Proposed structure of the crystalline phase appeared in the aged Fe-P-C alloys, where lamellae with a thickness D are piled densely along x-direction and L is the lamellar spacing.

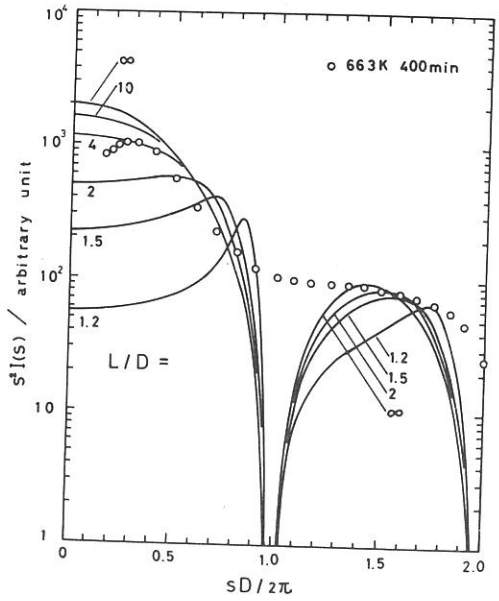

Fig.10 Relative change of $s^2I(s)$ as a function of $sD/2\pi$.

Table 2 Summary on the structure of the intially crystallized phase where D and L are the lamellar thickness and iter-lamellar spacing, respectively.

Ageing Condition		From Porod's Theory		From Correlation Function	
T /K	t /min	D /nm	L /nm	D /nm	L /nm
663	400	5.0	17.0	5.1	14.4
643	5000	4.5	14.0	4.6	16.6
643	10000	4.8	22.0	6.0	18.6

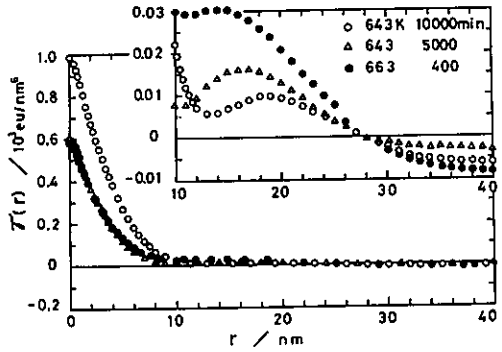

Fig.11 Electron density-density correlation in the aged specimens containing fine particles with lamellar structure in Fe-P-C alloys.

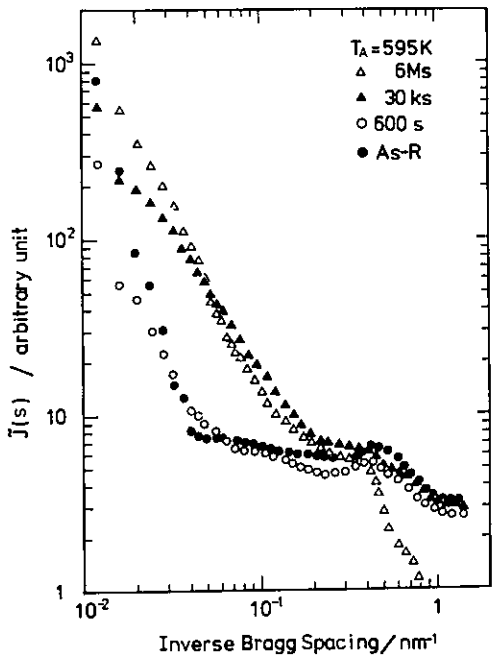

Fig.12 Change of SAXS intensity during ageing at 595 K in Fe-B alloys.

Table 3 Size parameters of crystalline α phase appeared during ageing at 653 K in Pd-Au-Si alloys.

Ageing Time /s	R_G /nm	Diameter from TEM /nm
600	5.3	-
1800	5.3	-
3600	5.9	7.0
7200	9.4	14.0

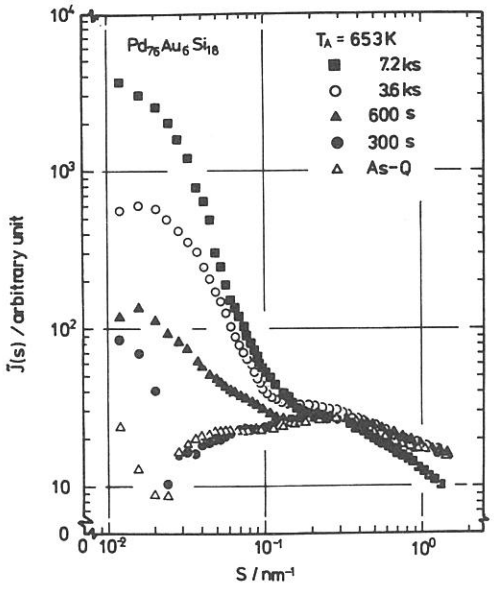

Fig.13 Change of SAXS intensity during ageing at 653 K in Pd-Au-Si alloys.

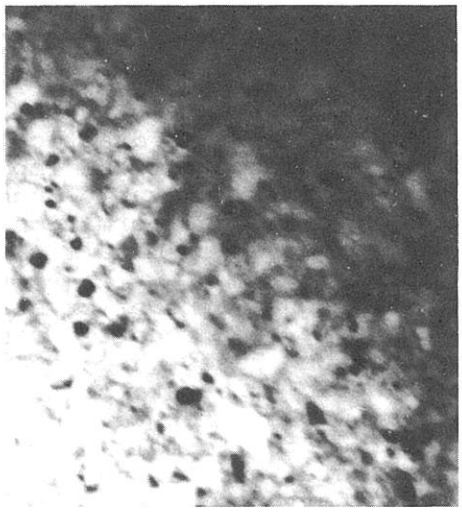

Fig.14 TEM photograph for the Pd-Au-Si alloy aged at 653 K for 7.2 ks. (x90,000)